

Koopman Theory for Partial Differential Equations

J. Nathan Kutz, Joshua L. Proctor and Steven L. Brunton

Abstract We consider the application of Koopman theory to nonlinear partial differential equations. We demonstrate that the observables chosen for constructing the Koopman operator are critical for enabling an accurate approximation to the nonlinear dynamics. If such observables can be found, then the dynamic mode decomposition algorithm can be enacted to compute a finite-dimensional approximation of the Koopman operator, including its eigenfunctions, eigenvalues and Koopman modes. Judiciously chosen observables lead to physically interpretable spatio-temporal features of the complex system under consideration and provide a connection to manifold learning methods. We demonstrate the impact of observable selection, including kernel methods, and construction of the Koopman operator on two canonical, nonlinear PDEs: Burgers' equation and the nonlinear Schrödinger equation. These examples serve to highlight the most pressing and critical challenge of Koopman theory: a principled way to select appropriate observables.

1 Introduction

Data-driven mathematical methods are increasingly important for characterizing complex systems across the physical, engineering, social and biological

J. N. Kutz

Department of Applied Mathematics, University of Washington, Seattle, WA 98195-3925, e-mail: kutz@uw.edu

J. L. Proctor

Institute for Disease Modeling, 3150 139th Ave SE, Bellevue, WA 98005, e-mail: joproctor@intven.com

S. L. Brunton

Department of Mechanical Engineering, University of Washington, Seattle, WA 98195, e-mail: sbrunton@uw.edu

sciences. These methods aim to discover and exploit a relatively small subset of the full space where low-dimensional models can be used to describe the evolution of the system. Thus solutions can often be approximated through dimensionality reduction methods where if n is the dimension of the original high-dimensional system, and r is the dimension of the subspace (or slow-manifold) where the dynamics is embedded, then $r \ll n$. The reduced order modeling (ROM) community has used this to great effect in applications such as large-scale patterns of atmospheric variability [1], turbulent flow control architectures [2] and/or spatio-temporal encodings in neurosensory systems [3]. Traditionally, the large-scale dynamics may be embedded in the low-dimensional space using, for instance, the proper orthogonal decomposition (POD) in conjunction with Galerkin projection. More recently, the dynamic mode decomposition (DMD), and its Koopman generalization, have garnered attention due to the fact that they can (i) discover low-rank spatio-temporal patterns of activity, and (ii) they can embed the dynamics in the subspace in an equation-free manner, unlike the Galerkin-POD method of ROMs. In this manuscript, we demonstrate that the Koopman architecture can yield accurate low-dimensional embeddings for nonlinear partial differential equations (PDEs). Critical to its success is an appropriate choice of observables, which is demonstrated to act as a nonlinear manifold learning method. We demonstrate the success of the method, and compare it to traditional DMD, on two canonical PDE models: Burgers' equation and the nonlinear Schrödinger equation.

Historically, the DMD method originated in the fluid dynamics community as a principled technique to decompose complex flows into a simple representation based on low-rank, spatio-temporal coherent structures. Schmid and Sesterhenn [4] and Schmid [5] first defined the DMD algorithm and demonstrated its ability to provide physically interpretable insights from high-dimensional fluids data. The growing success of DMD stems from the fact that it is an *equation-free*, data-driven method capable of providing an accurate decomposition of a complex system into spatio-temporal coherent structures that may be used for diagnostic analysis, short-time future state prediction, and control. Importantly, Rowley *et al.* [6] showed that DMD is connected to the underlying nonlinear dynamics through Koopman operator theory [7] and is readily interpretable using standard dynamical systems techniques [8, 9, 10, 11]. Specifically, the DMD algorithm is a manifestation of Koopman theory when the observable functions are the identity or a linear transformations of the underlying state space. Thus DMD is a principled, algorithmic architecture allowing for an explicit approximation of the Koopman operator. For more details, there are numerous detailed references [6, 12, 13].

The approximation of the Koopman operator via DMD is critically important for enabling evaluation of the operator from data. Indeed, it transforms Koopman theory from an abstract mathematical conception to a readily tractable computation. It also highlights the important role played by observables and their associated evolution manifolds. In particular, nonlin-

ear PDEs can be thought to evolve on manifolds which are often difficult to characterize and are rarely known analytically. A correct choice of observables can, in some cases, *linearize* the nonlinear manifold. For instance, the nonlinear evolution governed by Burgers' PDE equation can be linearized by the Cole-Hopf transformation, thus providing a linear manifold which can trivially describe the evolution dynamics. Such exact solutions to nonlinear PDEs are extremely rare and do not often exist in practice, with the inverse scattering transform (IST) for Korteweg-deVries, nonlinear Schrödinger and other integrable PDEs being the notable exceptions. Regardless, judiciously chosen observables can help transform a PDE evolving on a strongly nonlinear manifold to a weakly nonlinear manifold, enabling a more accurate and broader range of applicability of the Koopman approximation.

2 Koopman Theory, Observables, and Dynamic Mode Decomposition

The original work of Koopman in 1931 [7] considered Hamiltonian systems and formulated the Koopman operator as a discrete-time mapping. We generalize the Koopman operator definition for a continuous time system.

Definition: Koopman Operator: *Consider a continuous-time dynamical system*

$$\frac{d\mathbf{x}}{dt} = \mathbf{f}(\mathbf{x}), \quad (1)$$

where $\mathbf{x} \in \mathcal{M}$ is the state on a smooth n -dimensional manifold \mathcal{M} . The Koopman operator \mathcal{K} is an infinite-dimensional linear operator that acts on all observable functions $g : \mathcal{M} \rightarrow \mathbb{C}$ so that:

$$\mathcal{K}g(\mathbf{x}) = g(\mathbf{f}(\mathbf{x})). \quad (2)$$

In the following year, Koopman and von Neumann extended these results to dynamical systems with continuous spectra [14]. Critical to implementing this definition numerically is understanding how to choose a finite set of observables $g(\mathbf{x})$. This remains an open challenge today and will be addressed in our PDE examples.

By construction, the Koopman operator is a *linear*, infinite-dimensional operator that acts on the Hilbert space \mathcal{H} of *all* scalar measurement functions g . The Koopman operator acts on functions of the state space of the dynamical system, trading nonlinear finite-dimensional dynamics for linear infinite-dimensional dynamics. It can be further generalized to map infinite-dimensional nonlinear dynamics to infinite-dimensional linear dynamics by appropriate choice of observables. In practice, the computation of the Koopman operator will require a finite-dimensional representation. The advantage

of the Koopman representation is compelling: linear problems can be solved using standard linear operator theory and spectral decompositions. With such methods the infinite dimensional representation is handled by considering a sufficiently large, but finite, sum of modes to approximate the Koopman spectral solution. It should be noted that the definition (2) can be alternatively represented by a composition of the observables with the nonlinear evolution: $\mathcal{K}g = g \circ \mathbf{f}$.

The Koopman operator may also be defined for discrete-time dynamical systems, which are more general than continuous-time systems. In fact, the dynamical system in (1) will induce a discrete-time dynamical system given by the flow map $\mathbf{F}_t : \mathcal{M} \rightarrow \mathcal{M}$, which maps the state $\mathbf{x}(t_0)$ to a future time $\mathbf{x}(t_0 + t)$:

$$\mathbf{F}_t(\mathbf{x}(t_0)) = \mathbf{x}(t_0 + t) = \mathbf{x}(t_0) + \int_{t_0}^{t_0+t} \mathbf{f}(\mathbf{x}(\tau)) \, \mathrm{d}\tau. \quad (3)$$

This induces the discrete-time dynamical system

$$\mathbf{x}_{k+1} = \mathbf{F}_t(\mathbf{x}_k), \quad (4)$$

where $\mathbf{x}_k = \mathbf{x}(kt)$. The analogous discrete-time Koopman operator is given by \mathcal{K}_t such that $\mathcal{K}_t g = g \circ \mathbf{F}_t$. Thus, the Koopman operator sets up a discrete-time dynamical system on the observable function g :

$$\mathcal{K}_t g(\mathbf{x}_k) = g(\mathbf{F}_t(\mathbf{x}_k)) = g(\mathbf{x}_{k+1}). \quad (5)$$

If an appropriate Koopman operator can be constructed, then linear operator theory provides the spectral decomposition required to represent the dynamical solutions of interest. Specifically, the eigenfunctions and eigenvalues of the Koopman operator \mathcal{K} give a complete characterization of the dynamics. We consider the eigenvalue problem

$$\mathcal{K}\varphi_k = \lambda_k \varphi_k. \quad (6a)$$

The functions $\varphi_k(\mathbf{x})$ are Koopman eigenfunctions, and they define a set of intrinsic measurement coordinates, on which it is possible to advance these measurements with a *linear* dynamical system. The low-dimensional embedding of the dynamics are ultimately extracted from the Koopman eigenfunctions. More precisely, a reduced-order linear model can be constructed by a rank- r truncation of the dominant eigenfunctions φ_k .

A vector of observables \mathbf{g} , which is in our new *measurement space*, may be expressed in terms of Koopman eigenfunctions φ as

$$\mathbf{g}(\mathbf{x}) = \begin{bmatrix} g_1(\mathbf{x}) \\ g_2(\mathbf{x}) \\ \vdots \\ g_p(\mathbf{x}) \end{bmatrix} = \sum_{k=1}^{\infty} \varphi_k(\mathbf{x}) \mathbf{v}_k, \quad (7)$$

where \mathbf{v}_k is the k -th Koopman mode associated with the k -th Koopman eigenfunction φ_k , i.e. it is the weighting of each observable on the eigenfunction. In the original theory [7], Koopman considered Hamiltonian flows that are measure preserving, so that the Koopman operator is unitary. In this case, the eigenfunctions are all orthonormal, and (7) may be written explicitly as:

$$\mathbf{g}(\mathbf{x}) = \sum_{k=1}^{\infty} \varphi_k(\mathbf{x}) \begin{bmatrix} \langle \varphi_k, g_1 \rangle \\ \langle \varphi_k, g_2 \rangle \\ \vdots \\ \langle \varphi_k, g_p \rangle \end{bmatrix} = \sum_{k=1}^{\infty} \varphi_k(\mathbf{x}) \mathbf{v}_k. \quad (8)$$

The dynamic mode decomposition algorithm is used to compute an approximation to the Koopman eigenvalues λ_k and modes \mathbf{v}_k .

The nonlinear dynamical system defined by \mathbf{f} in (1) and the infinite-dimensional, linear dynamics defined by \mathcal{K} in (2) are equivalent representations of a dynamical system. One can either evolve the system in the original state space (1), requiring computational effort since it is nonlinear, or one can instead evolve using (2) and (7) so that the time dynamics are trivially computed

$$\mathcal{K}\mathbf{g}(\mathbf{x}) = \mathcal{K} \sum_{k=1}^{\infty} \varphi_k(\mathbf{x}) \mathbf{v}_k = \sum_{k=1}^{\infty} \mathcal{K}\varphi_k(\mathbf{x}) \mathbf{v}_k = \sum_{k=1}^{\infty} \lambda_k \varphi_k(\mathbf{x}) \mathbf{v}_k. \quad (9)$$

Thus future solutions can be computed by simple multiplication with the Koopman eigenvalue. Such a mathematical strategy for evolving nonlinear dynamical systems would seem always to be advantageous. However, it remains an open challenge how to systematically link the observables \mathbf{g} and the associated Koopman mode expansion to the original evolution defined by \mathbf{f} . For a limited class of nonlinear dynamics, this can be done explicitly [15].

Figure 1 illustrates the underlying concept in the Koopman approach. A dynamical system consisting of snapshots \mathbf{x}_k evolves according to the nonlinear dynamical system defined by \mathbf{F}_t in (4). In the state space, the nonlinearity generates a nonlinear manifold in which the data is embedded. The DMD approximation produces a least-square fit *linear dynamical system* approximating the flow map and the low-dimensional embedding (left panel of Fig. 1). Koopman theory ideally defines an operator that attempts to *linearize* the space in which the data is embedded. The Koopman operator then produces a linear flow map and low-dimensional embedding that approximates the full nonlinear dynamics (right panel of Fig. 1).

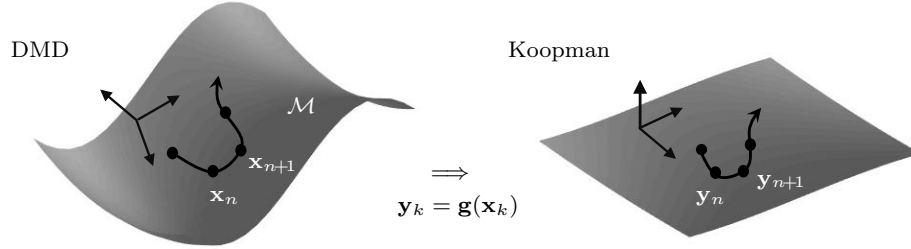


Fig. 1 The left panel illustrates the nonlinear manifold on which the dynamical system defined by \mathbf{F}_t in (4) generates a solution. DMD approximates the evolution on this manifold by a least-square fit linear dynamical system. In contrast, the selection of appropriate observables $g(\mathbf{x})$ define a Koopman operator that helps *linearize* the manifold so that a least-square fit linear dynamical system provides a much better approximation to the system (right panel).

3 The DMD and Koopman algorithms

The DMD algorithm underlies the computation of the Koopman eigenvalues and modes directly from data. Its effectiveness depends sensitively on the choice of observables. Rowley *et al.* [6] showed that DMD approximates the Koopman operator for the set of observables $\mathbf{g}(\mathbf{x}) = \mathbf{x}$. We will use this fact in constructing a DMD algorithm for observables of \mathbf{x} instead of the state variable itself. To start, we use the following definition of the DMD decomposition [12]:

Definition: Dynamic Mode Decomposition (Tu *et al.* 2014 [12]): Suppose we have a dynamical system (4) and two sets of data

$$\mathbf{X} = \begin{bmatrix} | & | & & | \\ \mathbf{x}_1 & \mathbf{x}_2 & \cdots & \mathbf{x}_m \\ | & | & & | \end{bmatrix} \quad (10a)$$

$$\mathbf{X}' = \begin{bmatrix} | & | & & | \\ \mathbf{x}'_1 & \mathbf{x}'_2 & \cdots & \mathbf{x}'_m \\ | & | & & | \end{bmatrix} \quad (10b)$$

with \mathbf{x}_k an initial condition to (4) and \mathbf{x}'_k it corresponding output after some prescribed evolution time Δt with there being m initial conditions considered. The DMD modes are eigenvectors of

$$\mathbf{A}_{\mathbf{X}} = \mathbf{X}'\mathbf{X}^\dagger \quad (11)$$

where \dagger denotes the Moore-Penrose pseudoinverse.

The above definition provides a computational method for evaluating the Koopman operator for a linear observable. In practice, three practical constraints must be considered: (i) We have data \mathbf{X} and \mathbf{X}' , but we do not necessarily know $\mathbf{F}_t(\cdot)$, (ii) We will have to make a finite-dimensional approximation to the infinite-dimensional Koopman operator \mathcal{K} , and (iii) We will have to judiciously select the observables $g(\mathbf{x})$ in order to have confidence that that Koopman operator will approximate the nonlinear dynamics of $\mathbf{F}_t(\cdot)$. Points (i) and (ii) go naturally together. Specifically, the number of measurements in each column of \mathbf{X} and \mathbf{X}' are n , while the number of total columns (time measurements) is m . Thus finite-dimensionality is imposed simply from the data collection limitations. The dimension can be increased with a large set of observables, or it can be decreased via a low-rank truncation during the DMD process. The observables are more difficult to deal with in a principled way. Indeed, a good choice of observables can make the method extremely effective, but it would also require expert knowledge of the system at hand [15]. This will be discussed further in the examples.

The following gives a practical demonstration of how to use the data, the DMD algorithm, and the observables to produce a Koopman operator and a future state prediction of the nonlinear evolution (1). The Koopman algorithm simply applies DMD on the space of observables.

1. From the data matrices \mathbf{X} and \mathbf{X}' , create the data matrices of observables \mathbf{Y} and \mathbf{Y}' :

$$\mathbf{Y} = \begin{bmatrix} | & | & & | \\ \mathbf{g}(\mathbf{x}_1) & \mathbf{g}(\mathbf{x}_2) & \cdots & \mathbf{g}(\mathbf{x}_{m-1}) \\ | & | & & | \end{bmatrix} \quad (12a)$$

$$\mathbf{Y}' = \begin{bmatrix} | & | & & | \\ \mathbf{g}(\mathbf{x}'_1) & \mathbf{g}(\mathbf{x}'_2) & \cdots & \mathbf{g}(\mathbf{x}'_{m-1}) \\ | & | & & | \end{bmatrix} \quad (12b)$$

where each column is given by $\mathbf{y}_k = \mathbf{g}(\mathbf{x}_k)$ or $\mathbf{y}'_k = \mathbf{g}(\mathbf{x}'_k)$

2. Perform the DMD algorithm on the pair \mathbf{Y} and \mathbf{Y}' to compute

$$\mathbf{A}_\mathbf{Y} = \mathbf{Y}'\mathbf{Y}^\dagger \quad (13)$$

along with the low-rank counterpart $\tilde{\mathbf{A}}_\mathbf{Y}$ obtained by projection onto a truncated POD subspace. The eigenvalues and eigenvectors of $\mathbf{A}_\mathbf{Y}$ may approximate Koopman eigenvalues and modes if the observables are well chosen.

3. DMD can be used to compute the augmented modes $\Phi_\mathbf{Y}$, which may approximate the Koopman modes, by

$$\Phi_Y = Y'V\Sigma^{-1}W \quad (14)$$

where W comes from the eigenvalue problem $\tilde{A}_Y W = W\Lambda$ and $Y = U\Sigma V^*$. Note that an r -rank truncation of the SVD is performed at this stage.

4. The future state in the space of observables is given by the linear evolution

$$y(t) = \Phi_Y \text{diag}(\exp(\omega t)) b \quad (15)$$

where $b = \Phi_Y^\dagger y_1$ is determined by projecting back to the initial data observable. The continuous-time eigenvalues ω are obtained from the discrete-time eigenvalues λ_k (i.e., diagonal elements of the matrix Λ) where $\omega_k = \ln(\lambda_k)/\Delta t$.

5. Transform from observables to state space

$$y_k = g(x_k) \rightarrow x_k = g^{-1}(y_k). \quad (16)$$

This last step is trivial if one of the observables selected to comprise $g(x_k)$ is the state variable x_k itself. If only nonlinear observables of x_k are chosen, then the inversion process can be difficult.

This process shows that the DMD algorithm is closely related to the Koopman operator. Indeed, it is the foundational piece for practical evaluation of the finite-dimensional Koopman operator. It is stressed once again here: selection of appropriate observables is critical for the algorithm to generate good reconstructions and approximations to the future state. We can also now introduce the following theorem [6, 12, 16, 17].

Theorem: Koopman and Dynamic Mode Decomposition: *Let φ_k be an eigenfunction of \mathcal{K} with eigenvalue λ_k , and suppose $\varphi_k \in \text{span}\{g_j\}$, so that*

$$\varphi_k(x) = w_1 g_1(x) + w_2 g_2(x) + \cdots + w_p g_p(x) = \mathbf{w} \cdot \mathbf{g} \quad (17)$$

for some $\mathbf{w} = [w_1 \ w_2 \ \cdots \ w_p]^T \in \mathbb{C}^p$. If $\mathbf{w} \in R(Y)$, where R is the range, then \mathbf{w} is a left eigenvector of A_Y with eigenvalue λ_k so that $\tilde{\mathbf{w}}^ A_Y = \lambda_k \tilde{\mathbf{w}}^*$.*

Thus the Koopman eigenvalues are the DMD eigenvalues provided (i) the set of observables is sufficiently large so that $\varphi_k(x) \in \text{span}\{g_j\}$ and (ii) the data is sufficiently *rich* so that $\mathbf{w} \in R(X)$. This directly shows that the choice of observables is critical in allowing one to connect DMD theory to Koopman spectral analysis. If this can be done, then one can simply take data snapshots of a finite-dimensional nonlinear dynamical system in time and re-parameterize it as a linear system in the observable coordinates, which is amenable to a simple eigenfunction (spectral) decomposition. This representation diagonalizes the dynamics and shows that the time evolution of each eigenfunction corresponds to multiplication by its corresponding eigenvalue.

4 Koopman Observables and Kernel Methods

The effectiveness of Koopman theory hinges on one thing: selecting appropriate observables. Once observables are selected, the previous section defines a DMD-based algorithm for computing the Koopman operator whose spectral decomposition completely characterizes the approximation. In the machine learning literature, observables are often thought of as *features*, and we will build upon this concept to generate appropriate observables. An important practical consideration becomes the computational cost in generating the DMD approximation as the number of rows in the matrices \mathbf{Y} and \mathbf{Y}' get progressively larger with each additional observable.

In the absence of expert-in-the-loop knowledge of the dynamical system, one might consider, for instance, the support vector machine (SVM) literature and associated kernel methods [18, 19, 20, 21] for feature selection (observables). The SVM architecture suggests a number of techniques for constructing the feature space $\mathbf{g}(\mathbf{x})$, with a common choice being the set of polynomials such that

$$g_j(x) = \{x, x^2, x^3, x^4, \dots, x^p\} . \quad (18)$$

Using a large number of polynomials can generate an extremely large vector of observables for each snapshot in time. This is closely related to the Carleman linearization technique in dynamical systems [22, 23, 24]. Alternatively, kernel methods have found a high degree of success using (i) radial basis functions, typically for problems defined on irregular domains, (ii) Hermite polynomials for problems defined on \mathbb{R}^n , and (iii) discontinuous spectral elements for large problems with block diagonal structures. Regardless of the specific choice of feature space, the goal is to choose a sufficiently rich and diverse set of observables that allow an accurate approximation of the Koopman operator \mathcal{K} . Instead of choosing the correct observables, one then simply chooses a large set of candidate observables with the expectation that a sufficiently diverse set will include enough features for an accurate reconstruction of the Koopman modes, eigenfunctions and eigenvalues, which intrinsically characterize the nonlinear dynamical system.

Williams *et al.* [17, 25] have recently capitalized on the ideas of machine learning by implementing the so-called extended DMD and kernel DMD method on extended observables (18) within the DMD architecture. Moreover, they have developed an efficient way to compute $\tilde{\mathbf{A}}_{\mathbf{Y}}$ even for a large observable space. The kernel DMD method is the most relevant in practice as the number of observables (features) can rapidly grow so as to make n extremely high-dimensional. In the context of the Koopman operator, the kernel trick [18, 19, 20, 21] will define a function $h(\mathbf{x}, \mathbf{x}')$ that can be related to the observables $g_j(\mathbf{x})$ used for constructing \mathbf{Y} and \mathbf{Y}' . Consider the simple example of a quadratic polynomial kernel

$$h(\mathbf{x}, \mathbf{x}') = (1 + \mathbf{x}^T \mathbf{x}')^2 \quad (19)$$

where \mathbf{x} and \mathbf{x}' are data points in \mathbb{R}^2 . When expanded, the kernel function takes the form

$$\begin{aligned} h(\mathbf{x}, \mathbf{x}') &= (1 + x_1 x'_1 + x_2 x'_2)^2 \\ &= \left(1 + 2x_1 x'_1 + 2x_2 x'_2 + 2x_1 x_2 x'_1 x'_2 + x_1^2 x_1'^2 + x_2^2 x_2'^2\right) \\ &= \mathbf{Y}^T(\mathbf{x}') \mathbf{Y}(\mathbf{x}) \end{aligned} \quad (20)$$

where $\mathbf{Y}(\mathbf{x}) = [\sqrt{2}x_1 \ \sqrt{2}x_2 \ \sqrt{2}x_1 x_2 \ x_1^2 \ x_2^2]^T$. Note that for this case, both the Koopman observables and the kernel function (19) are equivalent representations that are paired together through the expansion (20). The so-called kernel trick posits that (19) is a significantly more efficient representation of the polynomial variables that emerge from the expansion (20). Instead of defining the Koopman observables $g_i(\mathbf{x})$, we instead define the kernel function (19) as it provides a compact representation of the feature space and an implicit computation of the inner products required for the Koopman operator.

The computational advantages of the kernel trick are considerable. For example, a polynomial kernel of degree p acting on data vectors \mathbf{x} and \mathbf{x}' in \mathbb{R}^n is given by

$$h(\mathbf{x}, \mathbf{x}') = (1 + \mathbf{x}^T \mathbf{x}')^p \quad (21)$$

which requires a single computation of the inner product $\alpha = \mathbf{x}^T \mathbf{x}'$. This requires $\mathcal{O}(n)$ and produces $f(\mathbf{x}, \mathbf{x}') = (1 + \alpha)^p$ where α is a constant. The resulting computational cost for this p th degree polynomial kernel remains $\mathcal{O}(n)$. In contrast, the equivalent observable space using \mathbf{Y} requires construction of a vector of length $\mathcal{O}(n^2)$ taking the form

$$\mathbf{Y}(\mathbf{x}) = [1 \ x_1 \ \cdots \ x_n \ x_1^2 \ x_1 x_2 \ \cdots \ x_n^2 \ \cdots \ x_1^p \ \cdots \ x_n^p]^T. \quad (22)$$

Computing the inner product $\mathbf{Y}^T(\mathbf{x}') \mathbf{Y}(\mathbf{x})$ is a significantly larger computation than the kernel form (21). Thus the kernel trick enables an advantageous representation of the various polynomial terms and circumvents the formation and computation associated with (22).

The choice of kernel is important and in practice, is not robust for Koopman methods. Some standard choices are often used, including the three most common kernels of SVM-based data methods:

$$\text{polynomial kernel (degree } p) \quad h(\mathbf{x}, \mathbf{x}') = (a + \mathbf{x}^T \mathbf{x}')^p \quad (23a)$$

$$\text{radial basis functions} \quad h(\mathbf{x}, \mathbf{x}') = \exp(-a|\mathbf{x} - \mathbf{x}'|^2) \quad (23b)$$

$$\text{sigmoid kernel} \quad h(\mathbf{x}, \mathbf{x}') = \tanh(\mathbf{x}^T \mathbf{x}' + a). \quad (23c)$$

The advantage of the kernel trick is quite clear, providing a compact representation of a very large feature space. For the polynomial kernel, for instance, a 20th-degree polynomial ($p = 20$) using (23a) is trivial and does not compute all the inner products directly. In contrast, using our standard Koopman observables $g(\mathbf{x}_j)$ would require one to explicitly write out all the terms generated from a 20th-degree polynomial on an n -dimensional data set, which is computationally intractable for even moderately large n . The tuning parameter a must be carefully chosen in practice for reasonable results.

In practice, the observables for \mathbf{Y} are implicitly embedded in the kernel $h(\mathbf{x}, \mathbf{x}')$. Specifically, we consider the observable matrix elements defined by

$$\mathbf{Y}^T \mathbf{Y}'(j, k) = h(\mathbf{x}_j, \mathbf{x}'_k) \quad (24)$$

where the (j, k) denotes the j th row and k th column of the correlation matrix, and the \mathbf{x}_j and \mathbf{x}'_k are the j th and k th columns of data. The kernel DMD formulation still requires the computation of the matrices \mathbf{V} and $\mathbf{\Sigma}$ which can be produced from $\mathbf{Y}^* \mathbf{Y} \mathbf{V} = \mathbf{\Sigma}^2 \mathbf{V}$. As before, the matrix elements of $\mathbf{Y}^* \mathbf{Y}$ are computed from $\mathbf{Y}^* \mathbf{Y}(j, k) = h(\mathbf{x}_j, \mathbf{x}_k)$. Thus all the required inner products are computed by projecting directly to the feature space. Note that if the linear kernel function $h(\mathbf{x}, \mathbf{x}) = \mathbf{x}^T \mathbf{y}$ is chosen, the kernel DMD reduces to the standard DMD algorithm.

5 Application to PDEs

To demonstrate the Koopman operator concepts, we apply the methodology to two illustrative and canonical PDEs: Burgers' equation and the nonlinear Schrödinger equation. With these two examples, we can (i) illustrate a scenario where the Koopman operator can exactly (analytically) linearize a dynamical system, (ii) demonstrate how to judiciously select observables, and (iii) show that kernel methods are highly sensitive as an observable selection technique.

5.1 Burgers' Equation

To demonstrate the construction of a specific and exact Koopman operator, we consider the canonical nonlinear PDE: Burgers' equation with diffusive regularization. The evolution, as illustrated in Fig. 2(a), is governed by diffusion with a nonlinear advection [26]:

$$u_t + uu_x - \epsilon u_{xx} = 0 \quad \epsilon > 0, \quad x \in [-\infty, \infty]. \quad (25)$$

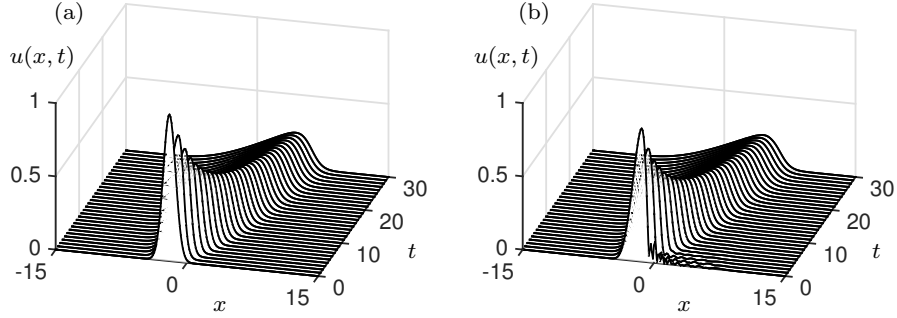


Fig. 2 (a) Evolution dynamics of Burgers' equation with initial condition $u(x,0) = \exp(-(x+2)^2)$. (b) Fifteen mode DMD approximation of the Burgers' evolution.

When $\epsilon = 0$, the evolution can lead to shock formation in finite time. The presence of the diffusion term regularizes the PDE, ensuring continuous solutions for all time.

Burgers' equation is one of the few nonlinear PDEs whose analytic solution form can be derived. In independent, seminal contributions, Hopf [27] and Cole [28] derived a transformation that linearizes the PDE. The Cole-Hopf transformation is defined as follows

$$u = -2\epsilon v_x / v. \quad (26)$$

The transformation to the new variable $v(x,t)$ replaces the nonlinear PDE (25) with the linear, diffusion equation

$$v_t = \epsilon v_{xx} \quad (27)$$

where it is noted that $\epsilon > 0$ in (25) in order to produce a well-posed PDE.

The diffusion equation can be easily solved using Fourier transforms. Fourier transforming in x gives the ODE system

$$\hat{v}_t = -\epsilon k^2 \hat{v} \quad (28)$$

where $\hat{v} = \hat{v}(k,t)$ denotes the Fourier transform of $v(x,t)$ and k is the wavenumber. The solution in the Fourier domain is easily found to be

$$\hat{v} = \hat{v}_0 \exp(-\epsilon k^2 t) \quad (29)$$

where $\hat{v}_0 = \hat{v}(k,0)$ is the Fourier transform of the initial condition $v(x,0)$.

To construct the Koopman operator, we can then combine the transform to the variable $v(x,t)$ from (26)

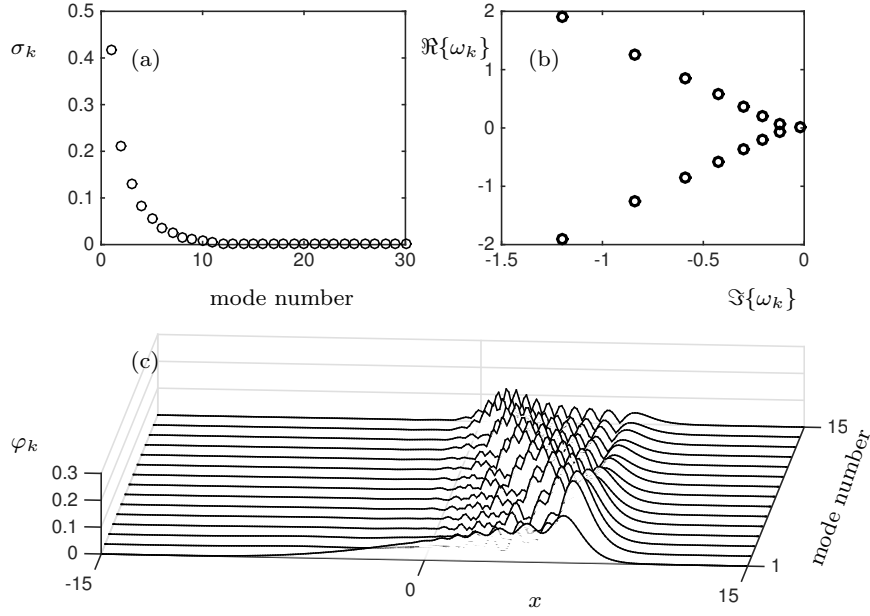


Fig. 3 DMD of the Burgers' equation. (a) The singular value spectrum demonstrates that a rank $r = 15$ truncation should be adequate to capture the dynamics of the front propagation in Fig. 2. (b) The eigen-decomposition in the DMD algorithm produces a DMD spectra whose eigenvalues are decaying. (c) The DMD modes used for reconstructing the solution in Fig. 2 ordered according the smallest to largest (in magnitude) eigenvalues. The first mode is like a *background* mode since the eigenvalue is almost zero.

$$v(x, t) = \exp \left[-\frac{\int_{-\infty}^x u(\xi, t) d\xi}{2\epsilon} \right] \quad (30)$$

with the Fourier transform to define the observables

$$g(u) = \hat{v}. \quad (31)$$

The Koopman operator is then constructed from (29) so that

$$\mathcal{K} = \exp(-\epsilon k^2 t). \quad (32)$$

This is one of the rare instances where an explicit expression for the Koopman operator and the observables can be constructed analytically. The inverse scattering transform for other canonical PDEs, KdV and NLS, also can lead to an explicit expression for the Koopman operator, but the scattering transform and its inversion are much more difficult to construct in practice.

To make comparison between Koopman theory and DMD, we consider the DMD method applied to governing equation (25). Applying the algorithm of Sec. 3 to the observables $g(\mathbf{x}) = \mathbf{x}$ gives the DMD approximation to the Burgers' dynamics as shown in Fig. 2(b). For this simulation, data snapshots were collected at intervals of $\Delta t = 1$ for the time range $t \in [0, 30]$. The singular value decay for the dynamics is shown in Fig. 3(a), suggesting that a rank $r = 15$ truncation is appropriate. The DMD spectra and DMD modes are illustrated in Fig. 3(b) and (c) respectively. Thus using $u(x, t)$ directly as an observable produces a low-rank model with fifteen modes. In contrast, by working with the observable (31), the Koopman operator can be trivially computed (32) and the dynamics analytically produced without need of approximation. In this case, the Koopman operator exactly linearizes the dynamics. This is the ideal which is hoped for, but rarely achieved with nonlinear PDEs (or nonlinear dynamical systems in general).

5.2 Nonlinear Schrödinger Equation

The example of Burgers' equation was easy to quantify and understand since the Cole-Hopf transformation was discovered nearly seven decades ago. Thus the observables chosen were easily motivated from knowledge of the analytic solution. Unfortunately, it is rarely the case that such linearizing transformations are known. In our second example, we consider the Koopman operator applied to a second canonical nonlinear PDE: the nonlinear Schrödinger equation

$$iu_t + \frac{1}{2}u_{xx} + |u|^2u = 0 \quad (33)$$

where $u(x, t)$ is a function of space and time modeling slowly-varying optical fields or deep water waves, for instance. Discretizing in the spatial variable x , we can Fourier transform the solution in space and use a standard time-stepping algorithm, such as a fourth-order Runge-Kutta, to integrate the solution forward in time.

As with Burgers' equation, we can compute the DMD by collecting snapshots of the dynamics over a specified time window. Specifically, we consider simulations of the equation with initial data

$$u(x, 0) = 2\text{sech}(x) \quad (34)$$

over the time interval $t \in [0, \pi]$. Twenty one snapshots of the dynamics are collected during the evolution, allowing us to create the snapshot matrix \mathbf{X} and \mathbf{X}' . The DMD reconstruction of the dynamics is demonstrated in Fig. 4(a). The low-rank DMD reconstruction provides a good approximation to the dynamics of the PDE.

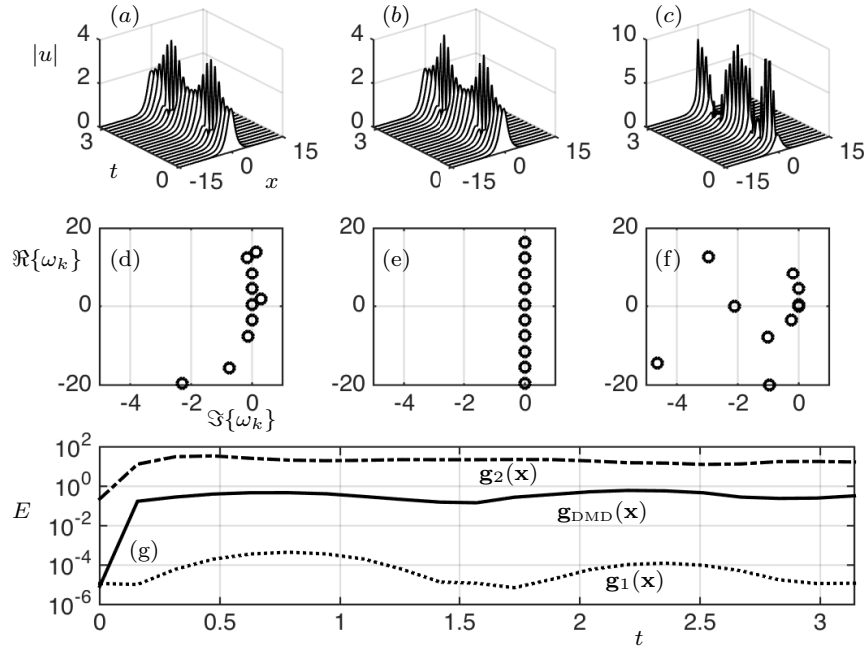


Fig. 4 Reconstruction of the NLS dynamics using (a) a standard DMD approximation $\mathbf{g}_{\text{DMD}}(\mathbf{x})$, (b) the NLS motivated $\mathbf{g}_1(\mathbf{x})$ and (c) a quadratic observable $\mathbf{g}_2(\mathbf{x})$. The Koopman spectra for each observable is demonstrated in panels (d), (e) and (f) which accompany the observables of (a), (b) and (c) respectively. Note that the observable $\mathbf{g}_1(\mathbf{x})$ produces a spectra which is approximately purely imaginary which is expected of the 2-soliton evolution. The error between the three observables and the full simulation is shown in panel (g). Note that the observable $\mathbf{g}_1(\mathbf{x})$ gives an error reduction of four orders of magnitude over DMD, while $\mathbf{g}_2(\mathbf{x})$ is an order of magnitude worse. This highlights the importance of selecting good observables.

To be more precise, it is explicitly assumed in the DMD reduction that the observables are simply the state variables \mathbf{x} where $\mathbf{x} = u(x, t)$ at discrete space and time points. The DMD observables are then given by

$$\mathbf{g}_{\text{DMD}}(\mathbf{x}) = \mathbf{x}. \quad (35)$$

Thus as previously noted, the DMD approximation is a special case of Koopman. The DMD spectrum for a rank $r = 10$ approximation is shown in Fig. 4(d). An ideal approximation would have the eigenvalues aligned along the imaginary axis since the evolution with the initial condition given by (34) is known as the 2-soliton solution which is purely oscillatory.

Koopman theory allows us a much broader set of observables. In what follows, we consider two additional observables

$$\mathbf{g}_1(\mathbf{x}) = \begin{bmatrix} \mathbf{x} \\ |\mathbf{x}|^2 \mathbf{x} \end{bmatrix} \quad (36a)$$

$$\mathbf{g}_2(\mathbf{x}) = \begin{bmatrix} \mathbf{x} \\ |\mathbf{x}|^2 \end{bmatrix}. \quad (36b)$$

The first observable $\mathbf{g}_1(\mathbf{x})$ is motivated by the form of the nonlinearity in the NLS equation. The second, $\mathbf{g}_2(\mathbf{x})$, is chosen to have a simple quadratic nonlinearity. It has no special relationship to the governing equations. Note that the choice of the observable $|\mathbf{x}|^2$ in $\mathbf{g}_2(\mathbf{x})$ is relatively arbitrary. For instance, one could consider instead $|\mathbf{x}|^5 \mathbf{x}$, \mathbf{x}^2 , \mathbf{x}^3 or \mathbf{x}^5 , for instance. These all produce similar results to the $\mathbf{g}_2(\mathbf{x})$ selected in (36b). Specifically, the observable $\mathbf{g}_2(\mathbf{x})$ is inferior to either the DMD or judiciously selected $\mathbf{g}_1(\mathbf{x})$ for the Koopman reconstruction.

As has been repeatedly stated, the success of the Koopman decomposition relies almost exclusively on the choice of observables. To demonstrate this in practice, we compute the Koopman decomposition of the NLS equation (33) using the two observables (36). The required data matrices have $2n$ rows of data, and only the state variables need to be recovered at the end of the procedure. Note that the algorithm produces both a state approximation since the first n components are actually the state vector \mathbf{x} , as well as approximations to the nonlinearity. The Koopman eigenfunctions and eigenvalues provide information about the evolution on the observable space.

Figure 4(b) and (d) show the Koopman reconstruction of the simulated data for the observables (36). The observable $\mathbf{g}_1(\mathbf{x})$ provides an exceptional approximation to the evolution while $\mathbf{g}_2(\mathbf{x})$ is quite poor. Indeed, the error of the DMD approximation and two nonlinear observables (36) are shown in Fig. 4(g) where the following error metric is used:

$$E(t_k) = \|\mathbf{x}(t_k) - \tilde{\mathbf{x}}(t_k)\| \quad k = 1, 2, \dots, m \quad (37)$$

where \mathbf{x} is the full simulation and $\tilde{\mathbf{x}}$ is the DMD or Koopman approximation. With the choice of observable $\mathbf{g}_1(\mathbf{x})$, which was judiciously chosen to match the nonlinearity of the NLS, the Koopman approximation of the dynamics is four-orders of magnitude better than a DMD approximation. A poor choice of observables, given by $\mathbf{g}_2(\mathbf{x})$, gives the worse performance of all, an order of magnitude worse than DMD. Note also the difference in the Koopman spectral as shown in the middle panels of Fig. 4. In particular, note that the judicious observables $\mathbf{g}_1(\mathbf{x})$ aligns the eigenvalues along the imaginary axis as is expected from the dynamics. It further suggests that much better long-time predictions can be achieved with the Koopman decomposition using $\mathbf{g}_1(\mathbf{x})$.

Observable selection in this case was facilitated by knowledge of the governing equations. However, in many cases, no such expert knowledge is available, and we must rely on data. The kernel DMD method allows one to use the kernel trick to consider a vast range of potential observables. As already highlighted, the kernel method allows for an efficient method to consider a

large class of potential observables without making the observation vector $\mathbf{g}(\mathbf{x})$ computationally intractable. For instance, one can consider a radial basis function kernel

$$f(\mathbf{x}, \mathbf{x}') = \exp(-|\mathbf{x} - \mathbf{x}'|^2) . \quad (38)$$

The absolute value is important for the case of the NLS equation considered due to the nonlinear evolution of the phase. This radial basis function is one of the more commonly considered kernels. Other kernels that we might consider include the three following observables

$$f(\mathbf{x}, \mathbf{x}') = (1 + \mathbf{x}^T \mathbf{x}')^{20} \quad (39a)$$

$$f(\mathbf{x}, \mathbf{x}') = (a + |\mathbf{x}^T| |\mathbf{x}'|)^{20} \quad (39b)$$

$$f(\mathbf{x}, \mathbf{x}') = \exp(-\mathbf{x}^T \mathbf{x}') . \quad (39c)$$

The first function is the standard polynomial kernel of 20th degree. The second instead takes the absolute value of the variable in a polynomial in order to remove the phase and the third is a Gaussian kernel that uses the same inner product as the polynomial kernel.

These three new kernels are compared to each other and the radial basis function. Figure 5 shows the spectra generated by these four kernels along with a comparison to the Koopman spectra generated by $\mathbf{g}_1(\mathbf{x})$. Note the tremendous variability of the results based upon the choice of kernel. Indeed, it highlights the tremendous sensitivity and non-robust nature of the kernel method for selecting observables. The choice of kernel must be carefully selected for either the extended or kernel DMD to give anything reasonable. Cross validation techniques could potentially be used to select a suitable kernel for applications of interest. It could also ensure that overfitting of the data does not occur. In either case, this simple example should serve as a strong cautionary tale for using kernel techniques in Koopman theory unless results are carefully cross validated.

6 Outlook on Koopman Theory for PDEs

Koopman analysis is a remarkable theoretical architecture with applicability to a wide range of nonlinear dynamical systems and PDEs. It combines a number of innovations across disciplines, including dimensionality-reduction techniques, manifold learning, linear operator theory, and dynamical systems. Although the abstract architecture provides a tremendously compelling viewpoint on how to transform nonlinear dynamical systems to infinite-dimensional linear dynamics, significant challenges remain in positing an appropriate set of observables for construction of the Koopman operator. If good candidate observables can be found, then the DMD algorithm can be enacted to compute a finite-dimensional approximation of the Koopman op-

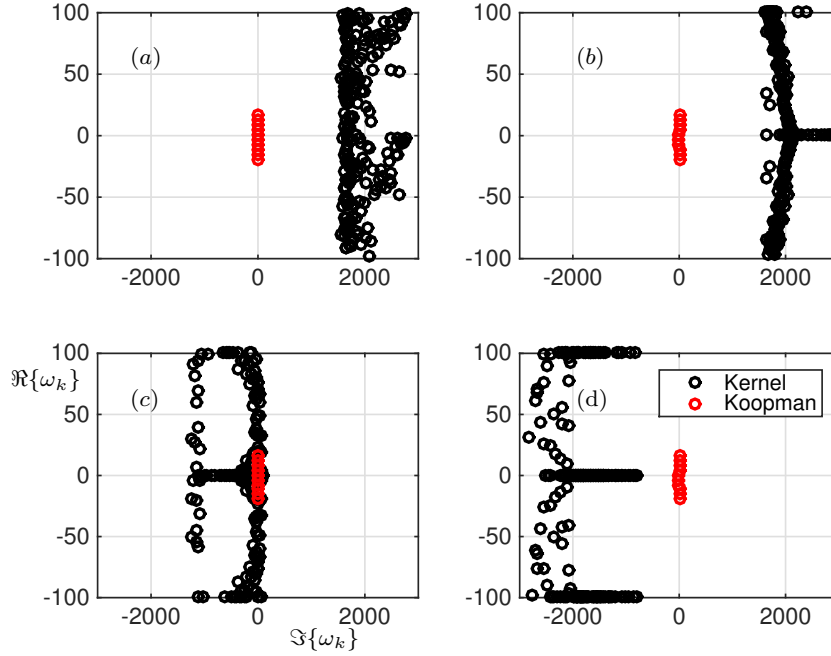


Fig. 5 Koopman spectra (a)-(d) of the four kernels considered in (38) and (39)(a)-(c) respectively. The red spectra is the Koopman spectra generated from the rank $r = 10$ observable $\mathbf{g}_1(\mathbf{x})$ which provides an exceptionally accurate reconstruction of the NLS dynamics.

erator, including its eigenfunctions, eigenvalues and Koopman modes. With a judicious choice of observables, these computed quantities can often lead to physically interpretable spatio-temporal features of the complex system under consideration.

We have demonstrated the application of Koopman theory on two canonical, nonlinear PDEs: Burgers' equation and the nonlinear Schrödinger equation. For Burgers' equation, the well-known Cole-Hopf transformation provides a critical link to an explicit calculation of the Koopman operator for a nonlinear PDE. Indeed, we show that the Koopman operator and associated observables can be trivially constructed from knowledge of the Cole-Hopf transformation. In contrast, choosing linear state observables for Burgers' yields a DMD approximation which is accurate, but lacks the clear physical interpretation of the exact Koopman reduction. Although the NLS equation can similarly be linearized via the inverse scattering transform, the transform and its inverse are technically difficult to compute for arbitrary initial conditions. Instead, we demonstrate that the selection of an observable that is motivated by the nonlinearity of the governing PDE gives a remarkably

accurate Koopman reduction. Indeed, the Koopman eigenfunctions and eigenvalues provide an approximation that is nearly equivalent to the accuracy of the numerical simulation itself. Importantly, for the NLS example, we also demonstrate that poor choices of observables are significantly worse than the DMD approximation. And for the case of observables chosen with a kernel method, the resulting spectra and eigenfunctions are highly inaccurate and non-robust, suggesting that such generic techniques as kernel methods may face challenges for use in observable selection.

Ultimately, the selected observables do not need to exactly linearize the system, but they should provide a method for transforming a strongly nonlinear dynamical system to a weakly nonlinear dynamical system. In practice, this is all that is necessary to make the method viable and informative. The results presented here are simultaneously compelling and concerning, highlighting the broader outlook of the Koopman method in general. Specifically, the success of the method will hinge on one issue: selection of observables. If principled techniques, from expert-in-the-loop knowledge, the form of the governing equation, or information about the manifold on which the data exists, can be leveraged to construct suitable observables, then Koopman theory should provide a transformative method for nonlinear dynamical systems and PDEs. We posit that sparse statistical regression techniques from machine learning may provide a path forward towards achieving this goal of selecting quality observables [29, 15]. Failing this, the Koopman architecture may have a limited impact in the mathematical sciences. Because of the importance of identifying meaningful observables, this is an exciting and growing area of research, especially given new developments in machine learning that may provide a robust and principled approach to observable selection.

Acknowledgements J. N. Kutz would like to acknowledge support from the Air Force Office of Scientific Research (FA9550-15-1-0385). J.L. Proctor would like to thank Bill and Melinda Gates for their active support of the Institute for Disease Modeling and their sponsorship through the Global Good Fund.

References

1. A. Majda. Challenges in climate science and contemporary applied mathematics. *Comm. in Pure and App. Mathematics*, 65:920–948, 2012.
2. S. L. Brunton and B. R. Noack. Closed-loop turbulence control: Progress and challenges. *Applied Mechanics Reviews*, 67:050801–1–050801–48, 2015.
3. S. Ganguli and H. Sompolinsky. Compressed sensing, sparsity, and dimensionality in neuronal information processing and data analysis. *Annual Review of Neuroscience*, 35:485–508, 2012.
4. P. J. Schmid and J. Sesterhenn. Dynamic mode decomposition of numerical and experimental data. In *61st Annual Meeting of the APS Division of Fluid Dynamics*. American Physical Society, November 2008.
5. P. J. Schmid. Dynamic mode decomposition of numerical and experimental data. *Journal of Fluid Mechanics*, 656:5–28, August 2010.

6. C. W. Rowley, I. Mezić, S. Bagheri, P. Schlatter, and D.S. Henningson. Spectral analysis of nonlinear flows. *J. Fluid Mech.*, 645:115–127, 2009.
7. B. O. Koopman. Hamiltonian systems and transformation in Hilbert space. *Proceedings of the National Academy of Sciences*, 17(5):315–318, 1931.
8. I. Mezić and A. Banaszuk. Comparison of systems with complex behavior. *Physica D: Nonlinear Phenomena*, 197(1–2):101 – 133, 2004.
9. I. Mezić. Spectral properties of dynamical systems, model reduction and decompositions. *Nonlinear Dynamics*, 41(1-3):309–325, 2005.
10. M. Budišić, R. Mohr, and I. Mezić. Applied Koopmanism a). *Chaos: An Interdisciplinary Journal of Nonlinear Science*, 22(4):047510, 2012.
11. I. Mezić. Analysis of fluid flows via spectral properties of the Koopman operator. *Annual Review of Fluid Mechanics*, 45:357–378, 2013.
12. J. H. Tu, C. W. Rowley, D. M. Luchtenburg, S. L. Brunton, and J. N. Kutz. On dynamic mode decomposition: theory and applications. *Journal of Computational Dynamics*, 1(2):391–421, 2014.
13. J. N. Kutz, S. L. Brunton, B. W. Brunton, and J. L. Proctor. *Dynamic Mode Decomposition: Data-Driven Modeling of Complex Systems*. SIAM, 2016.
14. B. O. Koopman and J. V. Neumann. Dynamical systems of continuous spectra. *Proceedings of the National Academy of Sciences of the United States of America*, 18(3):255, 1932.
15. S. L. Brunton, B. W. Brunton, J. L. Proctor, and J. N Kutz. Koopman observable subspaces and finite linear representations of nonlinear dynamical systems for control. *PLoS ONE*, 11(2):e0150171, 2016.
16. C. W. Rowley, M. O. Williams, and I. G. Kevrekidis. Dynamic mode decomposition and the Koopman operator: algorithms and applications. In *IPAM, UCLA*, 2014.
17. M. O. Williams, I. G. Kevrekidis, and C. W. Rowley. A data-driven approximation of the Koopman operator: Extending dynamic mode decomposition. *Journal of Nonlinear Science*, 25:1307–1346, 2015.
18. C. J. Burges. A tutorial on support vector machines for pattern recognition. *Data Mining and Knowledge Discovery*, 2:121–167, 1998.
19. S. Mika J. Ham, D. D. Lee and B. Schölkopf. A kernel view of the dimensionality reduction of manifolds. *Proceedings of the 21st International Conference on Machine Learning*, page 47, 2004.
20. B. Schölkopf T. Hofmann and A. Smola. Kernel methods in machine learning. *Annals of Statistics*, 36:1171–1220, 2008.
21. G. Baudat and F. Anouar. Kernel-based methods and function approximation. *Proceedings of the International Joint Conference on Neural Networks*, 2:1244–1249, 2001.
22. W.-H. Steeb and F. Wilhelm. Non-linear autonomous systems of differential equations and Carleman linearization procedure. *Journal of Mathematical Analysis and Applications*, 77(2):601–611, 1980.
23. K. Kowalski, W.-H. Steeb, and K. Kowalksi. *Nonlinear dynamical systems and Carleman linearization*. World Scientific, 1991.
24. S. P. Banks. Infinite-dimensional carleman linearization, the lie series and optimal control of non-linear partial differential equations. *International Journal of Systems Science*, 23(5):663–675, 1992.
25. M. O. Williams, C. W. Rowley, and I. G. Kevrekidis. A kernel approach to data-driven Koopman spectral analysis. *arXiv preprint arXiv:1411.2260*, 2014.
26. J. M. Burgers. A mathematical model illustrating the theory of turbulence. *Advances in applied mechanics*, 1:171–199, 1948.
27. E. Hopf. The partial differential equation $u_t + uu_x = \mu u_{xx}$. *Comm. Pure App. Math.*, 3:201–230, 1950.
28. J. D. Cole. On a quasi-linear parabolic equation occurring in aerodynamics. *Quart. Appl. Math.*, 9:225–236, 1951.

29. S. L. Brunton, J. L. Proctor, and J. N. Kutz. Discovering governing equations from data by sparse identification of nonlinear dynamical systems. *Proceedings of the National Academy of Sciences*, 113(15):3932–3937, 2016.